High Resolution Sequence Stratigraphy and its Implication in Mixed Siliciclastic Carbonate Sequence: A Case Study from Early to Middle Eocene Sylhet Formation, Assam and Assam-Arakan Basin, India*

Snehasis Chakrabarty[1], Dhritikanta Gorai[1], Monika Shukla[1], and S. Uppal[1]

Search and Discovery Article #30595 (2019)**
Posted January 28, 2019

*Adapted from extended abstract based on oral presentation given at 2018 International Conference and Exhibition, Cape Town, South Africa, November 4-7, 2018
 DOI:10.1306/30595Chakrabarty2019

[1]Keshav Deva Malaviya Institute of Petroleum Exploration, Oil and Natural Gas Corporation Ltd., 9 Kaulagarh Road, Dehradun-248001, Uttarakhand, India (chakrabarty_s@ongc.co.in)

Abstract

The Early to Middle Eocene 170 m thick Sylhet Formation of Assam and Assam-Arakan Basin belongs to an overall fining-upward 2nd order transgressive systems tract (TST). It consists of a mixed siliciclastic-carbonate sequence and the overall facies architecture implies deposition in a tide affected marginal marine (deltaic) to inner shelf carbonate ramp with episodic clastic supply from western hinterland by isolated protorivers during regressive phases. High resolution sequence stratigraphic analysis based on core and electrolog data allows to subdivide the 2nd order TST into 3 systems tracts of 3rd order, (i) basal TST, represented by shale and limestone followed by (ii) a highstand systems tract (HST) incorporating sandstone, limestone and shale, and (iii) a TST at the top. The HST can be further subdivided into 4th order parasequence-sets separated by marine flooding surfaces. The isopach and isolith maps of 4th order units as well as the conceptualized depositional model reveal a minimal sand supply at beginning of 3rd order HST and a significant increase in fluvial sand thereafter, resulting basinward progradation of facies and paleo shoreline due to a punctuated slow rise of relative sea-level that leads to constructive delta building until the end of 3rd order HST. The topmost 3rd order TST marks a landward retreat of facies due to paucity of sand supply and rise in relative sea-level.

As basin margin areas are more prone to periodic exposures related with lower order sea-level fluctuations, the secondary porosity development within sandstone and limestone has resulted due to percolation of meteoric water leading to significant dissolution of early formed calcite cement. Such phenomena are clearly evident by petrographic and SEM data and are helpful in finding the locales of better reservoir facies.

Sylhet Formation is characterized by abundant glauconitic horizons at selected stratigraphic levels that represent intervals of marine flooding events (MFE) of 3rd and 4th order sea-level change. The glauconites associated with MFE result in a condensed section with minimum sediment supply. The glauconitic horizons provide a key parameter to build the sequence stratigraphic architecture of the Eocene sequence. The depositional model and diagenetic events of such mixed siliciclastic-carbonate system are correlated, which helps explain the extent of short-term transgressive-regressive cycles, improving elucidation of hydrocarbon-bearing sand units for future exploration.

Introduction

High-resolution sequence stratigraphy (HRSS) deals with a scale of observation that typically falls below the resolution of seismic exploration methods, commonly referred to as lower order (4th-5th order) cycles. It is currently one of the potential areas of stratigraphic research, with a wide range of applications, from reservoir geology to tectonism and climate change (e.g., Galloway, 1989; Zecchin, 2005, 2007; Cantalamessa et al., 2007; Catuneanu et al., 2009; Zecchin et al., 2009, 2010, 2011; Csato et al., 2014). One of the key objectives of such analysis is to identify reservoir and source facies that are essential parts of a petroleum system. This article is focused on the Early to Middle Eocene Sylhet Formation in the North and South Assam Shelf (NAS and SAS) blocks of the Assam and Assam-Arakan Basin (A&AAB, Figure 1). So far, the dominantly carbonate Sylhet Formation has been interpreted as a carbonate ramp depositional system with development of sandstone near its top (Singh et al., 2011).

Paleogeographic reconstruction is based on faunal and floral evidence and lithological associations suggest widespread transgression during Early Eocene to Oligocene time, which was associated with accumulation of a 2nd order transgressive systems tract (TST) (Singh et al., 2011). However, such a TST is characterized by several small fining-upward and coarsening-upward cycles, within an overall fining-upward trend. Thus, identification of these high frequency cycles and corresponding sequence stratigraphic surfaces is felt necessary to bring out the changes in sedimentation pattern in the Sylhet Formation within a HRSS framework. The objective of this article is identification of high frequency sequences and depositional environments within the Early to Middle Eocene Sylhet Formation in the NAS and SAS blocks. The study will further enhance the understanding of variations in sediment supply and available accommodation within the Sylhet Formation in a much better way.

Geological Background

The A&AAB extends over large area of Northeast India, Myanmar and Bangladesh (Figure 1). Assam Shelf is located between the Eastern Himalayan foothills and the Assam-Arakan thrust belt. It is bounded by Mishmi Hills in northeast, Naga Hills to the southeast and Shillong Plateau and Mikir Hills basement uplift in south west. The A&AAB is subdivided into three major tectonic blocks (Figure 1) based on tectonic evolution and major basement faults, viz. North Assam Shelf (NAS), South Assam Shelf (SAS) and Assam and Assam-Arakan Fold Belt (AAFB). Lithostratigraphically, the NAS and SAS blocks are similar due to their same paleoenvironment of deposition and tectonic setting (Figure 2); the two blocks are separated by a strike-slip fault, widely known as Jorhat Fault (Evans, 1932; Dasgupta and Biswas, 2000). Sylhet Formation lies conformably over the Tura Formation, consists of mixed siliciclastic-carbonate sequence. The hydrocarbons are mostly present in the sandstone reservoirs restricted in the upper part of Sylhet Formation. The reservoir is adversely affected by cementation and other diagenetic changes which have posed challenge in proper evaluation of reservoir and selection of perforation intervals. The generalized lithostratigraphy of the Basin is summarised in Table 1.

Materials and Methods

The present work involves facies documentation of Sylhet Formation as well as laboratory investigations of the samples collected from cores and cuttings from 30 wells from different fields of NAS and SAS blocks (Figure 2; average thickness of studied intervals 120 m). Each

conventional core is of 6-9 m length with core diameter of 12.7 cm and more than 150 m of cores from different units of the Sylhet Formation were studied. Megascopic and petrographic studies have been carried out from cores and selected samples to identify and infer facies, microfacies, and mineral association, type of matrix/cement, texture and diagenetic imprints. Petrographic observations were carried out using a polarizing microscope using both transmitted and reflected light. Selected samples are analysed for clay mineralogy and bulk mineral identification by Rigaku Giergerflex X-ray diffractometer model ULTIMA-IV having a copper target. SEM-EDAX analysis of representative samples from the reservoir facies were analysed by GEOL JSM-5910LV to understand mineral composition, texture, clay minerals and reservoir characteristics. Basic electrolog data incorporating mainly four conventional logs; Gamma-Ray, Resistivity, Neutron and Density logs have been calibrated with lithology and the electrolog motifs were used for regional correlation (68 wells along 12 dip, and 2 strike profiles) of different units present within the Sylhet Formation. The sand thickness of individual parasequences have been measured from electrologs and plotted as sand isolith maps of lower orders in PETREL 2016 software M/S Schlumberger.

The cores have been studied in terms of their facies characteristics (Walker, 1984; Reading, 1996) to have a clear understanding of the process related facies analysis. These was further supported by regional correlation of electrologs from basin margin to interior and the sand isolith maps prepared for the lower order units, which reveal spatio-temporal changes in sedimentation pattern and 3-D sand distribution within the Sylhet Formation.

Facies Architecture and Depositional Setting

The Sylhet Formation (Early-Middle Eocene) of the A&AAB, India, consists of limestone, shale and sandstone-rich litho-units (Gupta et al., 2011). Though the Formation has been explored and exploited as an important hydrocarbon reservoir by ONGC, a detailed sedimentological analysis, particularly the different facies of Sylhet Limestone, has not been carried out so far. Thus, a detailed and systematic analysis of the Sylhet Formation was carried out. Such systematic documentation will signify the extent of marine incursions in the A&AAB during the Early to Middle Eocene time, which will provide better understanding of the reservoirs in the Sylhet Formation.

The Sylhet Limestone exhibits superposition of three distinct facies associations based on core studies, i.e. (i) Facies Association 1 (FA-1) consists of sandstone-mudstone-limestone heterolithic lower delta plain and shallow marine tidal flat deposits, (ii) Facies Association 2 (FA-2) having reddish, silty-shale and limestone dominated prodelta deposits, and (iii) Facies Association 3 (FA-3) with greenish grey shale rich pelagic-hemipelagic deposits, rich in fossil assemblages of foraminifera and nannoplanktons.

The sandstone-mudstone-limestone heterolithic facies association (FA-1) consists of four facies: argillaceous coarsening-up sandstone (1a), argillaceous fining-up sandstone (1b), wave ripple cross laminated sandstone (1c), coarse grained well sorted sandstone (1d), and sandstone-shale (1e), and shale-limestone heterolithic facies (1f) (Figure 3). All facies show variable sand: mud ratios with systematic change from sand to mud and mud to sand in vertical successions (Figure 3f). Petrographically, the sandstone is represented by quartz arenites with bimodal grain size distribution. All facies types are characterized by development of various tidally-generated structures, like flaser, lenticular and wavy bedding, tidal bundles with thin sand-shale alternations, double mud drapes and abundant bioturbations (Figure 3f, g, j), which indicate strong tidal influence within the inferred lower delta plain and delta front depositional system. Other structures occur due to the periodic change of tidal current directions, i.e., mutually opposite-oriented strata bundles and ripples with different orientations (Figure 3i) (e.g. Boersma, 1969;

Visser, 1980). Penecontemporaneously deformed mud laminae (Figure 3h) are also common. The coarsening-upward, sand-dominated facies represents mouth bars in a delta front setting, just seaward of the lower delta plain, while fining-upward sand-dominated facies with characteristic sedimentary structures suggest deposition in distributary channels. Mud and limestone-dominated and heterolithic facies indicate deposition in intertidal-subtidal flats within interdistributary bays/plains (Reading, 1996), indicating a lower delta plain depositional setting.

The silty-shale and limestone dominated prodelta association (FA-2) is represented by reddish to dark grey, carbonaceous shale (2a) and silty shale with sand/ silt lenses (2b) and wackestone to mudstone (2c) (Figure 4a-d). Dearth of coarser clastics, rarely preserved tidal features and abundant bioturbations within silty shale, indicate deposition in the relatively seaward part of the deltaic system (Nittrouer et al., 1986; Reading, 1996). The overall facies character, with predominance of grey, carbonaceous silty shale and sand/silt lenses points to a prodelta depositional setting.

The foraminifera and nannoplankton rich pelagic-hemipelagic association (FA-3) consists of greenish grey fissile shale (3a). These shales are greenish grey to pale grey, hard, moderately fissile, splintery at places and bioturbated towards their top and are associated with slikenslides (Figure 4e-f). In the upper part of the Sylhet Formation, the sandstones are separated by this shale facies that are regionally correlatable and show basinward (i.e., eastward) thickness increase (Figure 5a, b). The facies 3a is inferred to represent individual transgressive events with sheet-like geometry, coupled with paucity of coarser clastic supply and are identified as marine flooding intervals and are characterized by abundant calcareous nannoplankton, along with authigenic minerals such as glauconite and siderite (Pendkar et al., 2004). The facies correlation from basin margin to interior shows occurrence of FA-1 at several levels in the upper part of the Sylhet Formation, indicating facies progradation. The sediments, brought out by the Proto-river systems, were reworked by tidal processes. The coarsening-up sandstones show tidal imprints in terms of sandstone-mudstone alternations and bimodal grain population. The upward termination by the marine shales, followed by a younger sandstone unit, indicates large-scale marine flooding (Figure 5a, b).

Lower Order Sequences

3rd Order Units

The Sylhet Formation belongs to a 2nd order sequence consists of a TST (Lower to Upper Eocene) followed by HST (Oligocene) (Figure 6). This 2nd order TST is further subdivided into three major 3rd order systems tracts (Figure 7). The bottom part (~25 m thick) of the Sylhet Formation is devoid of sandstone and exhibits a fining-upward trend in log character, with maximum gamma values at its top, and represents a 3rd order TST bounded at its top by a MFS (Figure 7). The successive sandstone units above the basal TST exhibit a coarsening-up trend, constituting a 3rd order highstand systems tract (HST) (~80 m thick). This HST shows maximum sand distribution that indicates maximum rates of progradation and the top sandstone units represents a maximum regressive surface, marked as MRS_3rd-3 (MRS; Catuneanu, 2006). The overlying topmost unit consists of shale and limestone, shows a decline in sand and limestone thickness and is inferred to represent a retrogradation (TST) with fining-up log motifs represent the upper 3rd order TST (~20 m thick) (Figure 7). All three units are well correlatable in almost all the studied wells of NAS and SAS, commercial hydrocarbon accumulation is observed mostly in the Upper part of HST.

4th Order Units

In the present study, 4th order cycles have been identified based on high frequency marine flooding surfaces, corresponding to the high-frequency sequences of Catuneanu and Zecchin (2013). There are occurrences of three such marine flooding surfaces that can be laterally correlated within the 3rd order basal TST and overlying HST in drilled wells of NAS and SAS blocks. These are designated as FS_4th-1 to FS_4th-3 from below. FS_4th-1 divides the basal 3rd order TST into one 4th order TST unit (bounded by MRS_3rd-2 and FS_4th-1) and one 4th order HST+TST full unit (bounded by FS_4th-1 and MFS_3rd-3). Bottom 4th order TST unit mainly consists of shale with minor sandstone interbeds, whereas the overlying 4th order unit consists mainly of coarsening upward limestone with shale (Figure 5a, b). The marine flooding surfaces FS_4th-2 and FS_4th-3 divide the middle 3rd order HST into two 4th order parasequence-sets (full units) and one 4th order HST at the top (Figure 7). Each 4th order marine flooding surfaces can be laterally correlated from the basin margin to the interior (Fig. 5a,b). Sand distribution in each 4th order parasequence-set constituting the 3rd order HST shows a gradual increase in both thickness and lateral extent (Figure 5b) towards east (i.e. basinward). Isopach, sand isolith and facies maps are prepared for all the 4th order units within the 3rd order TST-HST which are described below (Figure 1, Figure 8, Figure 9, Figure 10, and Figure 11).

4th Order TST Unit (MRS_3rd -2 to FS-4th-1)

This sequence represents the initiation of first transgression with cessation of clastic input of Tura Formation and dominantly consists of shale with thin sandstone and limestone streaks.

4th Order HST-TST Unit-1 (FS_4th-1 to MFS_3rd-3)

From the sand isolith map, an isolated sand lobe around C-8 and M-1 has been identified (Figure 9), which may indicate the presence of a distributary mouth bar. Limestone has developed in inter-distributary areas (Figure 9). In a slightly deeper part, thick limestone bed is noticed with shale intercalations (L-2, P-1, M-1 and K-1). In the vicinity of Amguri and Charali area, this limestone directly overlies Tura sandstone while towards Panidihing and Lakwa fields, the limestone is separated from Tura Formation by a thin intervening shale. Thickness variation of this unit is shown in Figure 8. Coarsening upward trend of the limestone clearly indicates its deposition in a HST phase. Therefore, good secondary porosity development due to sub-aerial exposure within the limestone is a distinct possibility and this zone is known as Sylhet Pay.

4th Order HST-TST Unit-2 (MFS_3rd-3 to FS_4th-2)

Well-developed sandstones in wells F-1, G-1 and C-8 in SAS block indicate progradation due to more sediment supply (Figure 9). In NAS block, the sandstone is confined up to the North Rusdrasagar area. Limestone expansion has increased in SAS area due to non-supply of clastic sediments (Figure 9, and Figure 10). Thickness variation of this unit is shown in Figure 10b, c.

4th Order HST-TST Unit-3 (FS_4th-2 to FS_4th-3)

The occurrence of sand lobes in wells T-1, F-1 and N-1 in SAS and Panidihing area in NAS may indicate further progradation of the delta (Figure 1 and Figure 10), whereas the Khoraghat area is almost devoid of sandstone. In NAS, sandstone development has increased around North Rudrasagar area with regard to the lower unit. Lithologically, the producing zones consist of limestone-sandstone intercalations and show a coarsening upward trend in log motif.

4th Order top HST Unit (FS_4th-3 to MRS_3rd-3)

This unit shows maximum thickness of sandstone indicating highest sediment supply ensuring maximum progradation. The top surface is marked as MRS of 3rd order. Sandstone is well correlated in SAS area throughout all the wells (Figure 5a, b). Well-defined sand lobes present in wells T-1, M-2 and F-1 indicate constructive delta building. In NAS, extent of this sandstone has increased but thickness is in the range of 2-4 m. Good porosity development within sandstone and limestone might have developed in a much broader area along the 3rd order MRS due to its sub-aerial exposure. This sandstone unit is produced from a number of wells and the thickness variation of this sequence is shown in Figure 11a.

Electrolog Correlation

Electrolog correlation profiles in the Assam Shelf (NAS and SAS blocks) area are based on regional correlation of flooding surfaces of different ranks has enabled understanding the three dimensional distribution of the systems tracts, the lateral continuity of the marine flooding events and their landward counterparts, and allows building the depositional model of Sylhet Formation. The electrologs of wells have been studied with twelve dip (4 in NAS and 8 in SAS) and 2 strike profiles for log correlation. Two dip-aligned profiles in the northern part of NAS and SAS blocks show the basin margin to interior distribution of Sylhet sands in an east to west direction (Figure 5a, b). The Sylhet Formation belongs to part of the Early to Late Eocene TST of 2nd order. In the present study, the bottom surface of Sylhet Formation is marked as MRS_3rd-2 that also represents top of underlying Tura Formation.

The top of Sylhet is marked as MFS_3rd_4 on top of major drop of limestone growth indicating end of Sylhet Formation and thus indicating a drowning unconformity on top of Sylhet Formation (Figure 5a, b). In between MRS_3rd-2 and MFS_3rd-4 there are two another 3rd order surfaces, MFS_3rd-3 and MRS_3rd-3, which divide the total Sylhet into three 3rd order systems tracts, viz. lower TST, middle HST and followed by upper TST. Further 4th order subdivisions are based on regional correlation of lower order high frequency marine flooding surfaces. This has enabled understanding the three dimensional distribution of the systems tracts, the lateral continuity of the marine flooding events and allows to build-up the depositional model of the Early to Middle Eocene Sylhet Formation.

Isopach maps have been prepared for the Sylhet Formation (between MRS_3rd-2 and MFS_3rd-4) to show the thickness variations in NAS and SAS blocks (Figure 8). The maximum thickness of Sylhet occurs in the north-eastern part of NAS block (almost 160 m in Lakwa area) whereas minimum thickness occurs in the south-western part of SAS block (almost 40 m in Barpathar area). The basal 3rd order TST is a finning-upward cycle represented by increasing high gamma-ray and decreasing resistivity on log. Except Pandihing and Lakwa area the TST is considerably thin throughout the Assam Shelf. Thickness of this TST in NAS varies from 10-50 m, whereas in SAS it is in the range of 5- 25 m. Limestone, shale and sporadic sandstone are dominant facies.

The overlying 3rd order HST is characterized mainly by a coarsening up cycle (clearly observed in Lakwa and Khoraghat areas) with serrated log motif in the landward side (H-3 and G-1) of SAS as a result of clastic supply. During the HST period, the carbonate platform is well developed in south eastern part of SAS (in Khoraghat area) and in the north eastern part of NAS (in wells L-1, R-1, D-3). However, in the Panidihing, Amguri and Changmaigaon areas, limestone is poorly developed due to influx of finer clastics of prograding delta wedges. Sandstone is thickest at the top of this HST (Pie diagram is shown in Figure 11).

Topmost 3rd order TST mainly consists of fining upward thin limestone streaks within shale in NAS block and in Borholla and Khoraghat areas of SAS block. Both sandstone and limestone are developed in wells G-1, E-4, K-2 and T-1 in a fining upward fashion (Pie diagram is shown in Figure 5a, b).

Depositional Model

The producing zones of Sylhet are restricted either to the 3rd order regressive surface MRS_3rd-3 or to the regressive part of 4th order sequences. This suggests that the porosity pods were developed through subaerial exposure during relative fall in sea-level or basin-ward shifting of the paleoshoreline. The Lower unit of Sylhet Formation (3rd order lower TST), dominated by shale, witnessed a major transgressive event where almost the entire study area was under a subtidal environment. The lower unit of Sylhet Formation, comprised of thicker fining-upward trends and shorter coarsening-upward trends indicating longer durations of transgressive events followed by very smaller durations of regressive events (Figure 12). As a result of this, a large part of the study area was inundated, resulting in deposition of thick shale along with thin intervening buff to dirty white argillaceous micritic mudstone to wackestone (Figure 12a, b; TST part). In terms of sequence stratigraphy, the Lower Sylhet unit was deposited in a retrogradational ramp where the rate of accommodation space creation is greater than the sediment supply resulting in a rise of relative sea level and corresponding landward shift of the paleoshoreline. Presence of organic rich transgressive shales within the Lower Sylhet, as evident from petrographic analysis, suggests that these units are the major source pod that might have generated hydrocarbons in depositional lows. The thin limestone beds juxtaposed with the source pods, envisaged as products of smaller HST that developed within the progradational pulses, can be potential reservoirs. These limestone beds are referred to as Sylhet pay in the NAS Block where the gas bearing reservoirs are encased within the regressive phase of cycles. However, sandstone with shale intercalations is developed in Changpang, Merapani, Gankari and Harupani fields of SAS block during this period.

The Upper unit of Sylhet Formation (3rd order middle HST), deposited under a predominantly regressive phase is represented by thick limestone beds in the NAS block (Figure 12). Relatively clean carbonates (lesser argillaceous) with wackestone to packstone and intraclastic limestone facies with rounded limestone fragments (HST part) are expected in platformal areas (Figure 13c, d, e; e.g. Lakwa area, NAS). The limestone often display low angle stylolitic laminae observed within Sylhet Formation (Figure 13f, g). However in SAS block the facies is likely to be dominantly limestone-sandstone-shale alternations as a result of clastic interference from the hinterland (Figure 12). The top part of Sylhet Formation (3rd order upper TST) represents the fining upward thin limestone indicating cessation of carbonate platform (drowning unconformity) due to rapid rise in sea level. Based on the log motif and facies associations from core data it is inferred that Sylhet Formation is developed in a tide dominated deltaic set up in proximal part (eastern side of SAS block) and a stable carbonate platform in a distal part near Lakwa (NAS) and Khoraghat (SAS) area.

Implication of HRSS

Secondary Porosity Development

Complex diagenetic assemblage and paragenetic sequences can result if the paleodepositional environment changes as a result of relative sea level fluctuations prior to burial and isolation of sandstone unit (Curtis and Coleman, 1986). The Sylhet Formation was deposited in a tidal influenced shallow marine to carbonate ramp environment which are generally characterized by slightly alkaline waters (pH of seawater 8.3) and dominated by aqueous Na^{+} and Cl^{-} (with subordinate SO_4^{2-}, HCO_3^{-}, Ca^{2+} and Mg^{2+}) with salinity of 35 gpl. During deposition of Sylhet Formation, the lower order relative sea-level fluctuation controls the sequence building pattern and thus the diagenetic history and paragenetic sequence can be predicted. In Sylhet Formation, initial alkaline environment leads to intense early calcite cementation prior to mechanical compaction as evident from floating contacts and replacement of quartz by calcite along its periphery (Figure 14a). This early diagenetic carbonate cement has an exaggerated effect upon the porosity of sandstones because they locally fill pores or preferentially block pore throats. Dissolution of such early calcite cement as a result of meteoric diagenesis occurs within the regressive units and hence created good secondary porosity zones. Etched framework grains and remnant early calcite cement is confirmed from petrography and SEM in wells KT-3, B- 5, K-2, MK-7 and Y-1 (Figure 14a; Akhtar et al., 2004).

Since calcite cementation was strong enough to replace quartz (mostly along periphery), later grain dissolution has resulted in corroded outlines of grains with excellent preservation of secondary porosity in thin sections (Figure 14a, b). The zone of dissolution and development of secondary porosity within the Sylhet Formation can be predicted from the lower order sequence stratigraphic analysis, as this will be related with exposed areas landwards only where the initial alkaline environment is lost due to percolation of acidic meteoric water resulting in significant dissolution of early formed calcite cement. The secondary porosity created during the eogenesis stage as a result of meteoric diagenesis, however, is destroyed in many places through precipitation of authigenic kaolinite resulting from feldspar dissolution. In a few sandstones, presence of chlorite lining on corroded grain boundary of quartz strongly suggests that it has formed after dissolution of grain by calcite and creation of secondary porosity. It implies that authigenesis of chlorite has remained a continuous process both in early and late diagenetic stage. Hence, wide-spread dissolution of early formed calcite cements are related with events of lower order sea-level fall and are associated with such regressive surfaces and HRSS analysis are extremely helpful in finding the locales of better reservoir facies.

Occurrence and Significance of Glauconite

Sylhet Formation is characterized by abundant occurrences of glauconite at some specific stratigraphic intervals. The issue of modes of occurrence and significance of glauconite occurrences, especially with regard to its relationship with sequence stratigraphic surfaces has been addressed here on the basis of observation and data available from Sylhet Formation.

The glauconite has different degrees of maturity and occurs in three forms, viz. as altered form of fecal pellets, as infillings within bioclast-pores and as non-pellet stringers and blebs of glauconitic cements. Glauconite pellets appear as dark green or yellowish green with strong birefringence and pint point extinction under optical microscope. Pellets are rounded to sub-rounded (<0.8 mm), mostly entire and rarely

broken, moderate to poorly sorted and are characterized by smooth to slightly wrinkled surfaces (Figure 14c). The pellets exhibit deeply penetrating radiating cracks tapering inwards in most cases (Figure 14f).

Glauconite pellets appear as dark green or yellowish green with strong birefringence and pint point extinction under optical microscope. Pellets are rounded to sub-rounded (<0.8mm), mostly entire and rarely broken, moderate to poorly sorted and are characterized by smooth to slightly wrinkled surfaces (Figure 14c). The pellets exhibit deeply penetrating radiating cracks tapering inwards in most cases (Figure 14f). The yellowish green to grass green pellets with dull to earthy luster are relatively fresh, while matured pellets exhibit brownish green shiny appearance under transmitted light and in some extreme cases it turned into dark brown forming limonites. Euhedral framboidal pyrites may occur disseminated within the glauconitic pelloids. The glauconite infillings may be of two types, the most common variety occupies predominantly in the chambers, the canals and the tiny pores in the wall of bioclasts, while the second type of infilling occupies the intra-skeletal, open voids (Figure 14d). The glauconite is more matured within the fecal pellets and is less matured within the intraparticle pores of bioclasts. SEM-EDAX, XRD and geochemical studies clearly document that the glauconitic infilling within the intra-particle pores of bioclasts belong to nascent to slightly evolved variety (<5 wt% K), while the pellet belongs to slightly evolved to evolved glauconite (5-7 wt% K). Green stringers and blebs are also found within the intergranular spaces between framework grains in a few places (Figure 14e). Under the optical microscope, the glauconite appears as very fine pale green to yellowish green clayey material (Figure 14e). Under SEM, glauconite occurs as dense, uniform, and very fine flakes. The EDAX analysis shows the typical composition of glauconite with presence of Si, Al, Fe, and K.

Maturity of Sylhet Glauconite

The K content provides information about the maturity of glaucony (Odin and Matter, 1981) and shows a direct correlation with other attributes, such as the colour of grains. K-poor, nascent (K = 2-4%) and slightly evolved (K = 4-6%) glaucony has a pale to light green colour, with a few exceptions (Rao et al., 1995; McCracken et al., 1994) and generally shows obvious traces of the primary substrate of glauconitization. In contrast, evolved (K = 6- 8%) and highly evolved (K > 8%) glaucony, where substrate has been completely dissolved, is green to dark green. The Fe_2O_3 content of glaucony shows remarkably high values (up to 29%), and is higher than 15% also in the leastevolved samples. The SEM-EDAX analysis of glauconite bearing samples shows existence of all four types of glauconites based on its maturity.

Authigenic nature of the glauconitic pellets can be revealed by the presence of deep fractures at grain surfaces with fractured parts fitted together (Figure 14f; Bandopadhyay, 2007). The expansional growth of glauconite grains and possibly bioturbation of the sediment are likely to result in breakage of evolved to highly evolved grains (McCracken et al., 1994). In addition, fractures are characteristic of an advanced stage of glauconitization and have never been observed in nascent and slightly evolved glauconite (Giresse et al., 2015; Odin and Fullagar, 1988). Autochthonous origin of the glauconitic minerals is manifested by the generally higher degrees of roundness of the pelloids and the common association of the relatively finer feldspar grains (Amorosi, 1997). Also, the absence of broken pellets and the presence of deeply-penetrating fractures indicate the autochthonous origin of glauconite (Bandopadhyay, 2007; Banerjee et al., 2008, 2016).

Significance of Sequence Stratigraphic Analysis

In the present study, glauconite is found within Sylhet Limestone at different stratigraphic levels and is deposited in an intertidal shoreface to

innershelf environment. The Sylhet Formation has been subdivided into three third order system tracts, lower TST, middle HST and upper TST (Figure 5a, b). The lower TST and middle HST are again subdivided into 4th order high frequency units based on 4th order MFS (for details, see sequence stratigraphy). It has been observed that the occurrences of Glauconite are maximum at 3rd and 4th order MFS surfaces. Recent studies focusing on passive-margin successions during Sylhet times have shown that glauconite may be ubiquitous throughout a depositional sequence, but its origin, abundance, and maturity vary systematically within and through systems tracts. Maximum glauconite abundance and maturity are characteristics of the condensed section (CS) and the associated surface of maximum sediment starvation, which occur at the events of marine flooding intervals. Glauconite formation and maturation require prolonged residence at or near the sediment-water interface and hence is a reliable indicator of low sedimentation rate. The glauconitic horizons provide a key parameter to build the sequence stratigraphic architecture of Eocene sequence in the Assam and Assam-Arakan Basin.

Conclusions

This article provides the first systematic documentation of lower order, high frequency sequence stratigraphic elements within the Early to Middle Eocene Sylhet Formation of the Assam and Assam-Arakan Basin in the frame of its paleodepositional settings and paleogeography. The significant findings and conclusions are:

1) The Sylhet Formation is part of a 2nd order TST already recognized, which is analysed in the light of high-resolution sequence stratigraphy to identify 3rd order (TST/HST/TST) and 4th order (parasequence-sets) units, based on facies associations, trends of electrolog motifs and stratal packages.

2) Facies architecture reveals a basinward (eastward) progradation of delta plain deposits that follow the initial transgressive phase. The overall progradation was punctuated by lower order relative sea-level rise. Thereafter, again, a change to fining-upward in the upper part of Sylhet Formation manifests another transgression of the sea. The sand supply was considerably reduced and shale/limestone ratio increases. The Sylhet top is recognised as a drowning unconformity above which no limestone deposition took place. Eventually, the TST ends within the overlying Kopilli Formation. The study classifies a paleoslope towards the east and paleodrainage from the southwest, leading to the deposition of smaller deltaic lobes separated by broad inter-distributary bays.

3) The vertical stacking of lithounits within the Sylhet Formation indicates that the depositional model and paleogeographic reconstruction of 4th order units reveal minimal sand supply. The event was followed by a significant increase in sediment supply by the proto-river systems that led to progradation till the end of the HST (Sylhet sandstone units). The subsequent rise in relative sea-level resulted in retrogradation (3rd order TST) that continued during Kopilli Formation.

4) The 3rd order TST-HST-TST units of Sylhet Formation may be interpreted as the result of varying rates of rising RSL and sedimentation. The absence of RSL falls may have been favoured by continuous subsidence. The superimposed 4th order units also document varying rates of accommodation development and/or sedimentation.

5) HRSS analysis within the 3rd order HST towards the western basin margin provides a good match with the development of secondary porosity distribution along the lower order regressive surfaces, as this is more prone to sub-aerial exposure resulting in significant dissolution of early calcite cements, generation of secondary porosity and consequent structurally favorable entrapment condition.

6) Glauconites are ubiquitous within Sylhet Formation, though their occurrences are maximum at 3rd and 4^{th} order MFS surfaces. It is a reliable indicator of low sedimentation rate and thus maximum glauconite abundance and maturity are associated with surface of maximum sediment starvation, which occur at the events of marine flooding intervals. Therefore, glauconitic horizons provide a key parameter to build the sequence stratigraphic architecture of Eocene sequence in the Assam and Assam-Arakan Basin.

7) Such a high-resolution sequence stratigraphic model, depicting variations in sedimentation related to the extent of short-term marine transgressions and regressions, will definitely improve the knowledge of hydrocarbon-bearing limestone-shale-sandstone litho-successions in similar basins.

Acknowledgements

The authors are immensely grateful to Shri A.K. Dwivedi, Director (Exploration), ONGC for permission to publish the article. Thanks are due to Dr. Hari Lal, ED-HoI, KDMIPE, ONGC, for extending the support and facilities at KDMIPE. The views expressed in this article reflect the interpretation of the authors and may not necessarily represent the formal position of ONGC.

Selected References

Akhtar, M.S., et al., 2004, Microfacies analysis and distribution of reservoir sands of between Borholla and Khoraghat Fields, South Assam Shelf, p. 1-27.

Amorosi, A., 1997, Detecting compositional, spatial, and temporal attributes of glaucony: A tool for provenance research: Sedimentary Geology, v. 109, p. 135-153.

Bandopadhyay, P.C., 2007, Interpretation of authigenic vs. allogenic green peloids of ferric clay in the Proterozoic Penganga Group, southern India: Clay Minerals, v. 42, p. 471-485.

Banerjee, S., U. Bansal, and A.V. Thorat, 2016, A review on palaeogeographic implications and temporal variation in glaucony composition: J. Paleogeography, v. 5/1, p. 43-71.

Banerjee, S., S. Jeevankumar, and P.G. Eriksson, 2008, Mg-rich ferric illite in marine transgressive and highstand systems tracts: Examples from the Paleoproterozoic Semri Group, central India: Precambrian Research, v. 162, p. 212-226.

Boersma, J.R., 1969, Internal structure of some tidal mega-ripples on shoal in the Westerschelde estuary, the Netherlands: Report of a preliminary investigation: Geology en Mijnbou, v. 48, p. 409-414.

Cantalamessa, G., C.D. Celma, L. Ragaini, G. Valleri, and W. Landini, 2007, Sedimentology and high-resolution sequence stratigraphy of the late middle to late Miocene Angostura Formation (western Borbon Basin, north western Ecuador): J. Geol. Soc. London, v. 164, p. 653-665.

Catuneanu, O., 2006, Principles of Sequence Stratigraphy: Elsevier, Amsterdam, 386 p.

Catuneanu, O., V. Abreu, J.P. Bhattacharya, M.D. Blum, R.W. Dalrymple, P.G. Eriksson, C.R. Fielding, W.L. Fisher, W.E. Galloway, M.R. Gibling, K.A. Giles, J.M. Holbrook, R. Jordan, C.G.St.C. Kendall, B. Macurda, O.J. Martinsen, A.D. Miall, J.E. Neal, D. Nummedal, L. Pomar, H.W. Posamentier, B.R. Pratt, J.F. Sarg, K.W. Shanley, R.J. Steel, A. Strasser, M.E. Tucker, and C. Winker, 2009, Towards the standardization of sequence stratigraphy: Earth Science Reviews, v. 92, p. 1-33.

Catuneanu, O., and M. Zecchin, 2013, High-resolution sequence stratigraphy of clastic shelves II: Controls on sequence development: Marine and Petroleum Geology, v. 39, p. 26-38.

Coleman, J.M., and D.B. Prior, 1981, Deltaic environments of deposition, *in* Sandstone Depositional Environments, P.A. Scholle, and D. Spearing, eds., AAPG Memoir 31, p. 139-178.

Csato, I., O. Catuneanu, and D. Granjeon, 2014, Millennial-scale sequence stratigraphy: Numerical simulation with Dionisos: J. Sediment. Res., v. 84, p. 394-406.

Curtis, C.D., and M.L. Coleman, 1986, Controls on the precipitation of early diagenetic calcite, dolomite and siderite concretions in complex depositional sequences, *in* D.C. Gautier, ed., Roles of organic Matter in Sediment Diagenesis, Soc. Econ. Paleont. Miner Spec. Publ., v. 38, p. 23-33.

Dasgupta, A.B., and A.K. Biswas, 2000, Geology of Assam: Geological Society of India, Bangalore, 169 p.

Einsele, G., W., Ricken, and A. Seilacher, 1991, Cycles and Events in Stratigraphy: Springer-Verlag, Berlin, 955 p.

Evans, P., 1932, Tertiary Succession in Assam: Trans. Min. Geol. Metal. Inst. of India, v. 27/3, p.155-260.

Galloway, W.E., 1989, Genetic stratigraphic sequences in basin analysis I: architecture and genesis of flooding surface bounded depositional units: AAPG Bulletin, v. 73, p. 125-142.

Giresse, P., M.A. Bassetti, F. Chanier, V. Gaullier, A. Maillard, I. Thinon, J. Lofi, G. Lymer, J.-Y. Reynaud, A. Negri, and M. Saavedra-Pellitero, 2015, Depositional environment and age of some key Late Pliocene to Early Quaternary deposits on the underfilled Cedrino paleovalley (Orosei): Insight into the Neogene geodynamic evolution of Sardinia: Quaternary International, v. 357, p. 220-236.

Gupta, G.D., et al., 2011, Facies analysis and reservoir characterization of Tura/Sylhet, Kopili, Bokabil and Tipam based on conventional core/SWC study from Key wells of Dhansiri Valley covering Khoraghat, Golaghat, Nambar, Mirapani, East Lakhibari, Titabar and Borholla, p. 6-11.

McCracken, S.R., J. Compton, and K. Hicks, 1994, Sequence-stratigraphic significance of glaucony-rich lithofacies at Site 903, *in* G.S. Mountain, K.G. Miller, P. Blum, C.W. Poag, and D.C. Twichell, eds., Proceedings of the Ocean Drilling Program Leg 150 Scientific Results, Ocean Drilling Program, Texas A&M University, p. 171-187.

Nittrouer, C.A., S.A. Kuehl, D.J. DeMaster, and R.O. Kowsmann, 1986, The deltaic nature of Amazon shelf sedimentation: Bull. Geol. Soc. Am., v. 97, p. 444-456.

Odin, G.S., and P.D. Fullagar, 1988, Geological significance of the glaucony facies, *in* G.S. Odin, ed., Green Marine Clays: Developments in Sedimentology, v. 45, p. 295-332.

Pendkar, N., M.H. Basavaraju, P.S. Kataki, B. Jagtap and N.K. Borah, 2004, High resolution sedimentological and biostratigraphic studies on cored Sylhet and Tura formations of North Rudrasagar field, Upper Assam Shelf: ONGC unpublished report, RGL Sivasagar, Assam.

Rao, V.P., M. Thamban, and M. Lamboy, 1995, Verdine and glaucony facies from surficial sediments of the eastern continental margin of India: Marine Geology, v. 127, p. 105-113.

Reading, H., 1996, Sedimentary Environments: Processes, Facies and Stratigraphy, 3rd Edition, Wiley Blackwell, 704 p.

Singh, H.J., Md. S. Akhtar, A. Siawal, D. Chakravorty, and N. Kumar, 2011, Play and Prospectivity Analysis of Assam Arakan Basin: Unpublished ONGC Report, 118 p.

Swift, D.J.P., G.F. Oertel, R.W. Tillman, and J.A. Thorne, eds., 1991, Shelf Sand and Sandstone Bodies: Geometry, Facies and Sequence Stratigraphy: International Association of Sedimentologists Spec. Publ. 14, 532 p.

Van Wagoner, J.C., R.M. Mitchum, K.M. Campion, and V.D. Rahmanian, 1990, Siliciclastic sequence stratigraphy in well logs, cores, and outcrops: AAPG Methods in Exploration, no. 7, 55 p.

Visser, M. J., 1980, Neap Spring cycles reflected in Holocene subtidal large-scale bedform deposits, a preliminary note: Geology, v. 8, p. 543-546.

Walker, R.G., 1984, Facies Sequences and Facies Models: Geol. Assoc. Can., p. 317.

Zecchin, M., 2005, Relationships between fault-controlled subsidence and preservation of shallow-marine smallscale cycles: Example from the lower Pliocene of the Crotone Basin (southern Italy): J. Sediment. Res., v. 75, p. 300-312.

Zecchin, M., 2007, The architectural variability of small-scale cycles in shelf and ramp clastic systems: The controlling factors: Earth-Sci. Rev., v. 84, p. 21-55.

Zecchin, M., 2010, Towards the standardization of sequence stratigraphy: Is the parasequence concept to be redefined or abandoned?: Earth-Science Reviews, v. 102, p. 117-119.

Zecchin, M., D. Civile, M. Caffau, and C. Roda, 2009, Facies and cycle architecture of a Pleistocene marine terrace (Crotone, southern Italy): A sedimentary response to late Quaternary, high-frequency glacio-eustatic changes: Sediment. Geol., v. 216, p. 138-157.

Zecchin, M., M. Caffau, L. Tosi, D. Civile, G. Brancolini, F. Rizzetto, and C. Roda, 2010, The impact of Late Quaternary glacio-eustasy and tectonics on sequence development: Evidence from both uplifting and subsiding settings in Italy: Terra Nova, v. 22, p. 324-329.

Zecchin, M., D. Civile, M. Caffau, G. Sturiale, and C. Roda, 2011, Sequence stratigraphy in the context of rapid regional uplift and high-amplitude glacio-eustatic changes: The Pleistocene Cutro Terrace (Calabria, southern Italy): Sedimentology, v. 58, p. 442-477.

Zecchin, M., and O. Catuneanu, 2013, High-resolution sequence stratigraphy of clastic shelves I: Units and bounding surfaces: Marine Petrol. Geol., v. 39, p. 1-25.

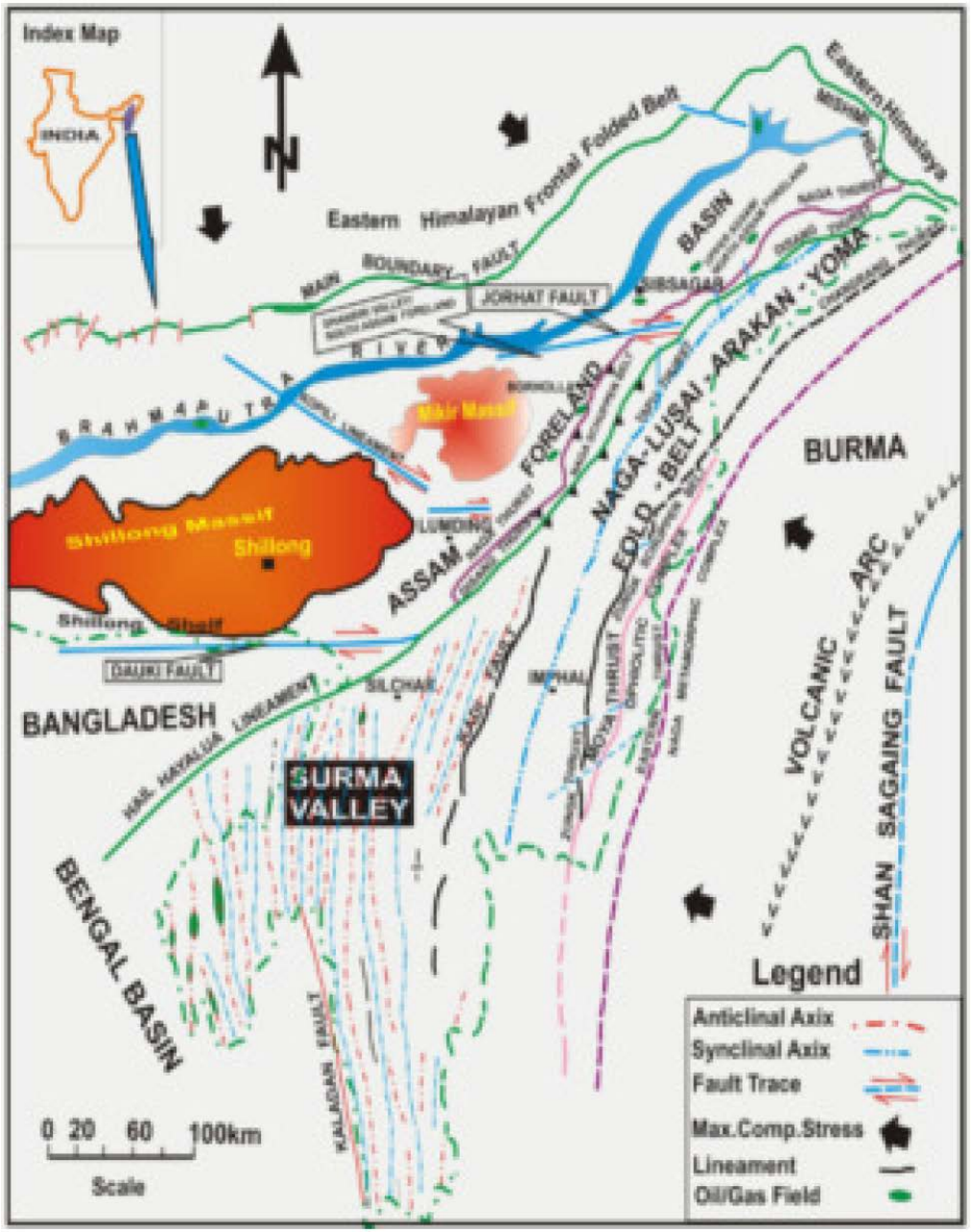

Figure 1. Tectonic map of Assam and Assam and Assam Arakan Basin.

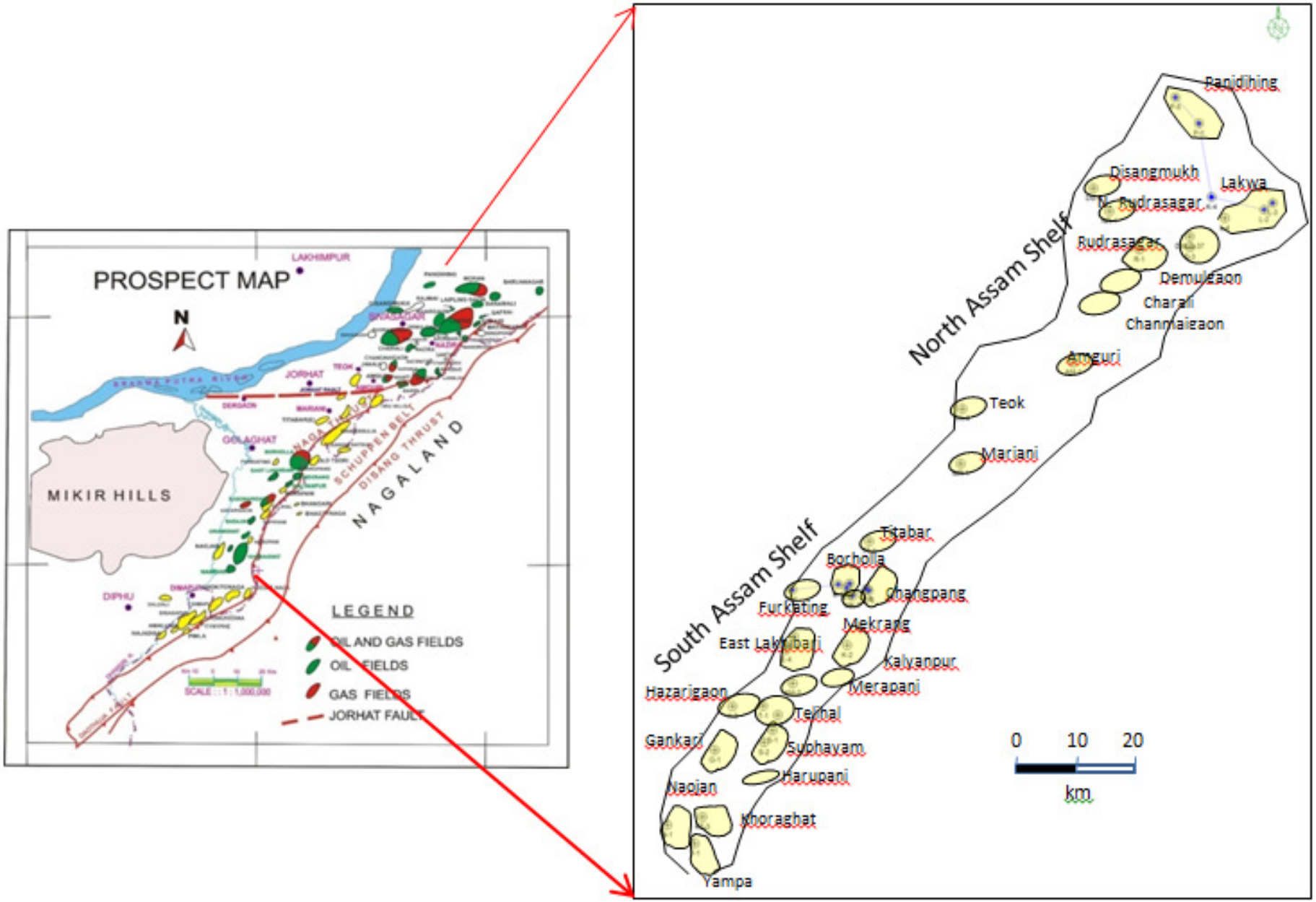

Figure 2. Location map of North and South Assam Shelf, Basin showing different fields.

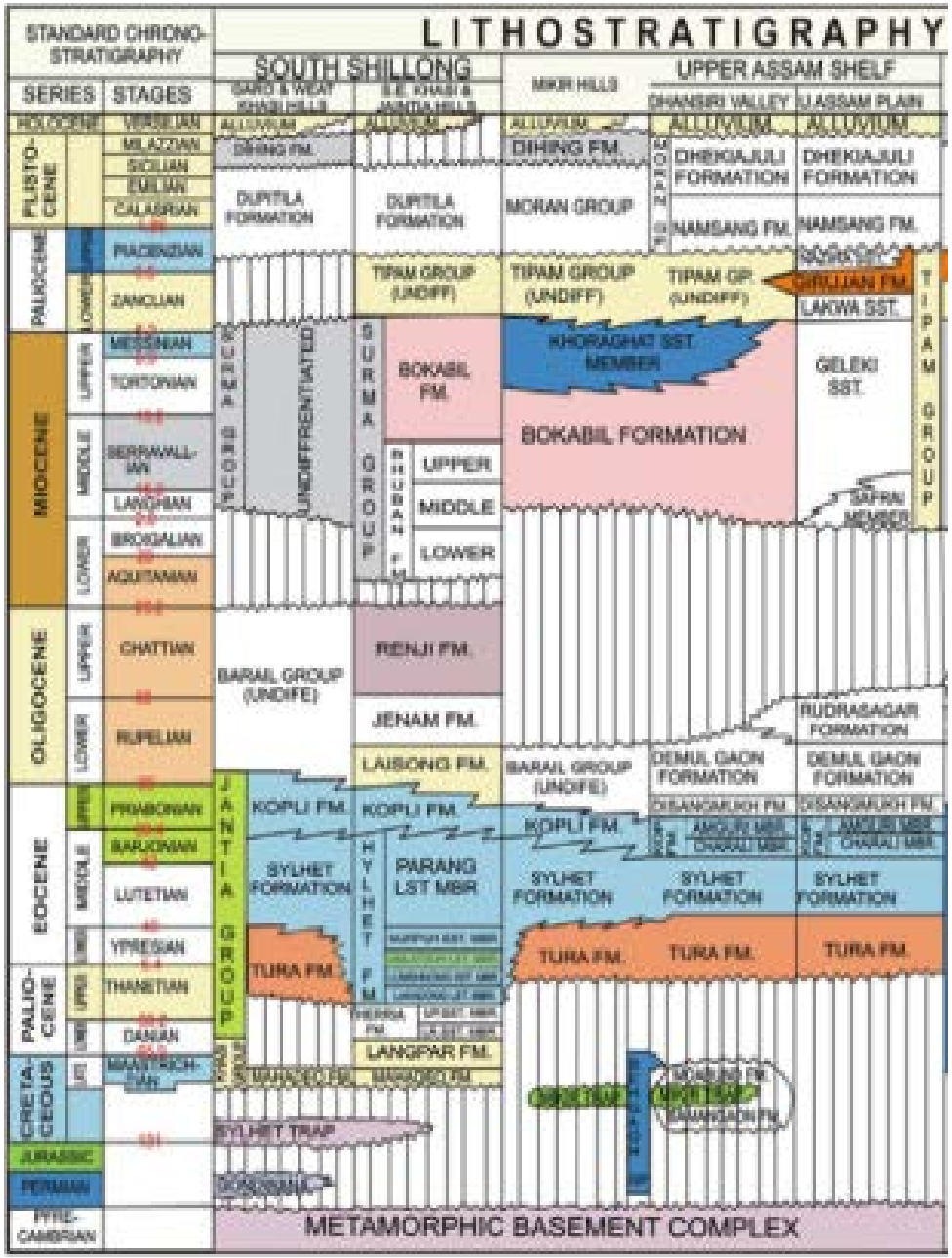

Table 1. Generalised stratigraphy of Assam and Assam Arakan Basin (after Pandey et al.,1997).

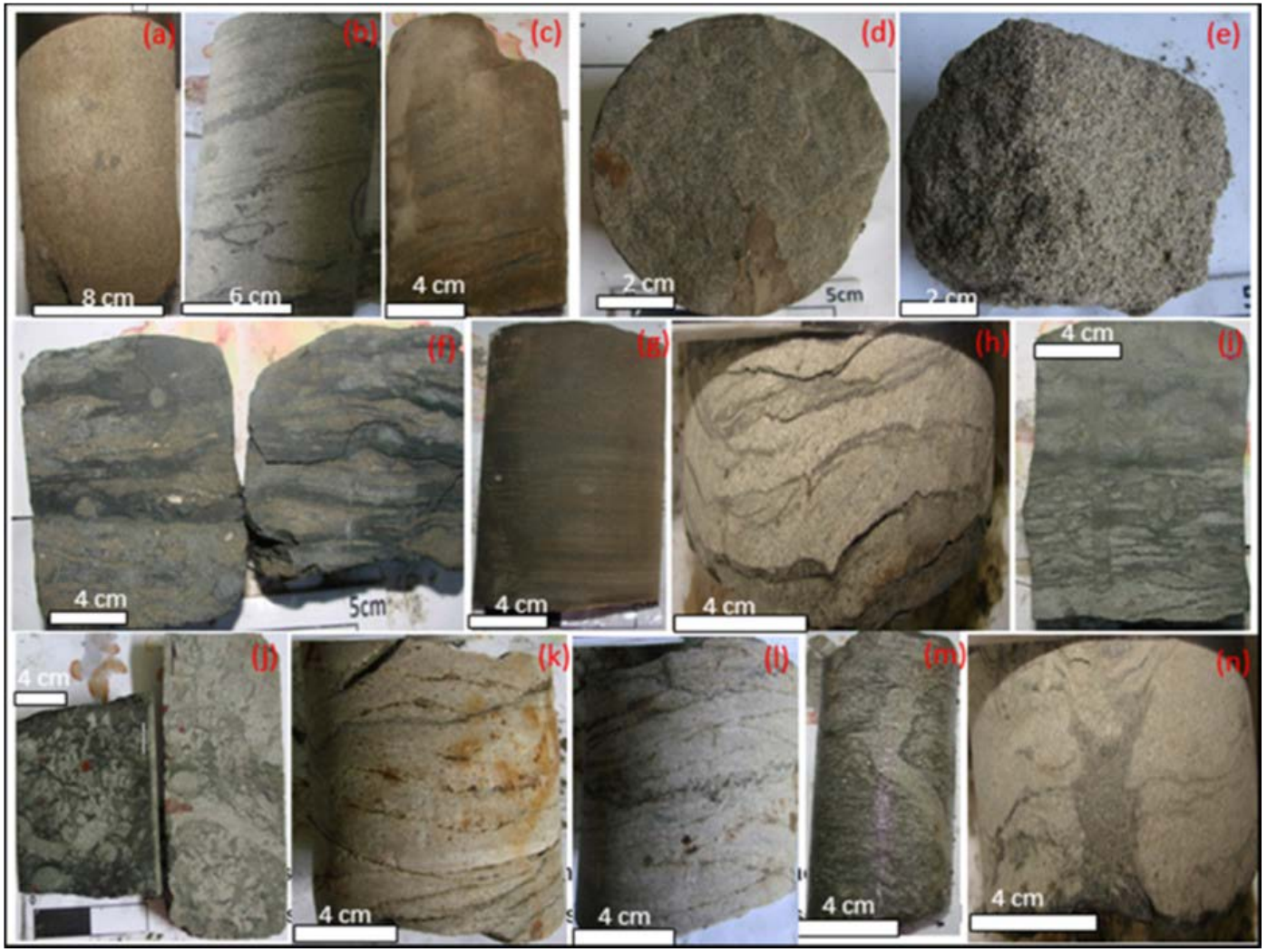

Figure 3. (a) Massive argillaceous sandstone, often fining up (facies 1b). (b and c) Cross-stratified fining-upward sandstone representing facies 1c, (d and e) Coarse-grained well-sorted sandstone characterised by facies 1d, (f) Sandstone-shale heterolith (facies 1e), note sharp change in lithology due to tidal fluctuations, (g) Rhythmic alternations of sandstone-shale laminae, note occurrences of double mud drapes, (h) Penecontemporaneously deformed mud laminae, (i) Heterolithic facies gradually changes into shale, note in the lower part bidirectional ripple laminations and thin flaser beds. (j) Profusely bioturbated heterolithic facies, (k and l) Wavy, ripple laminated sandstone (facies 1c), note bundle wise up-building and draping-offshooting wave ripple lamination, (m) Vertical skolithos burrows within bioturbated heterolithic facies (facies 3D), (n) Mud injection as a result of penecontemporaneous deformations.

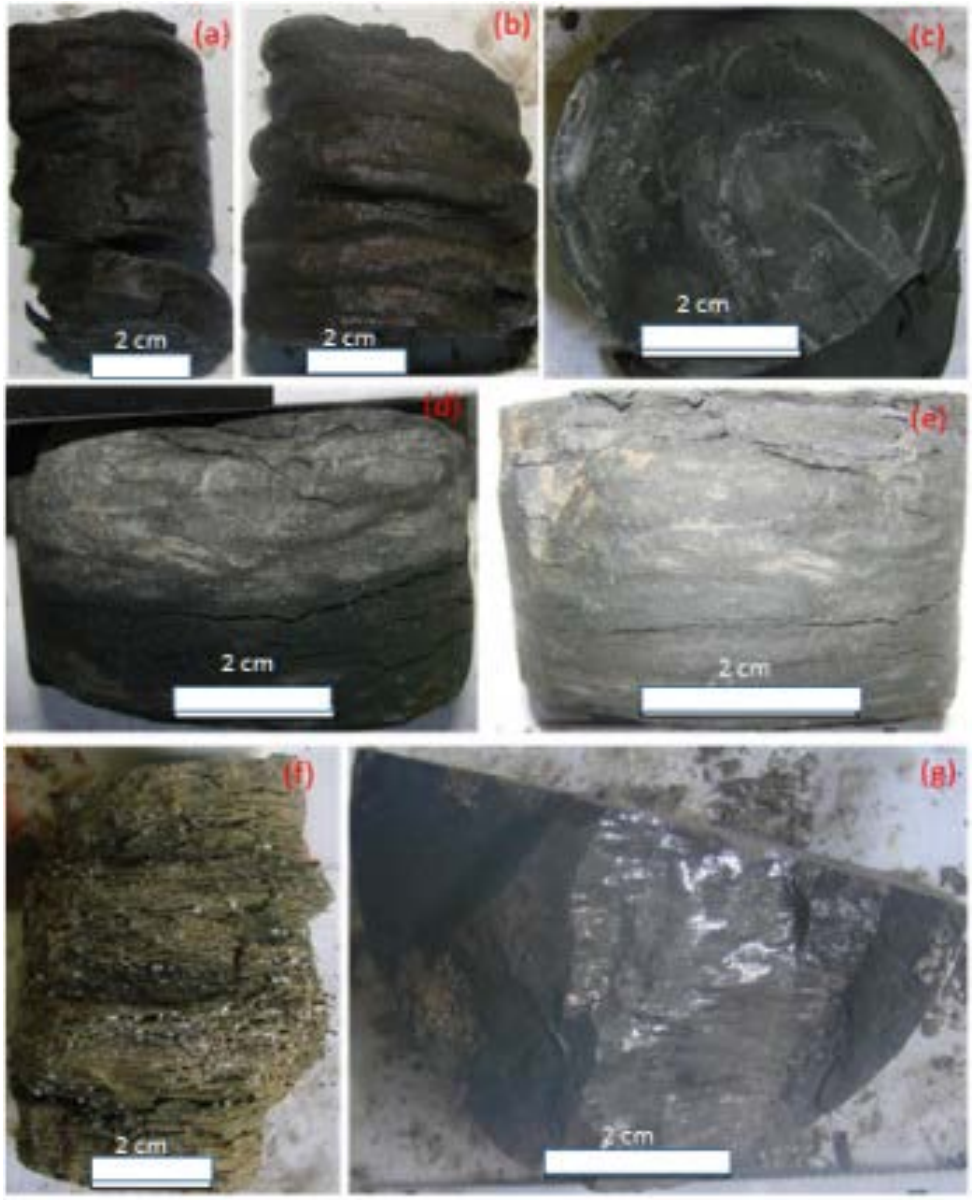

Figure 4. (a and b) Grey to reddish, hard, moderately to poorly fissile silty shale (facies 2a), (c) Carbonaceous shale with devoid of any tidal imprints (facies 2a), (d) Shale with sandstone/siltstone lenses (facies 2b), (e) Greenish to grey shale (facies 3a), (f) Occurrences of striated and polished slikenslides within facies 3a.

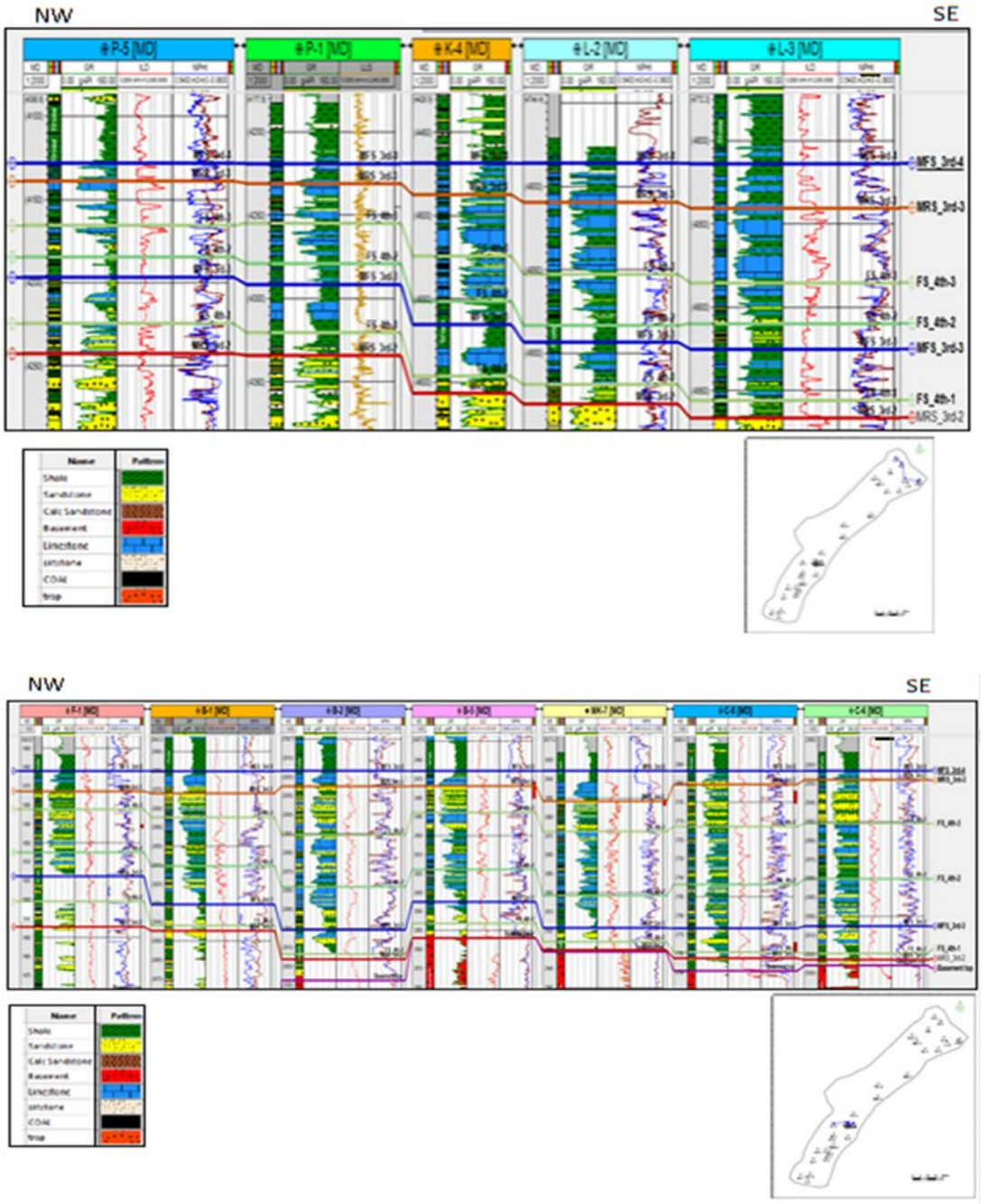

Figure 5. (a) Electrolog correlation and lithofacies distribution along dip profile (NAS). (b) Electrolog correlation and lithofacies distribution along dip profile (SAS).

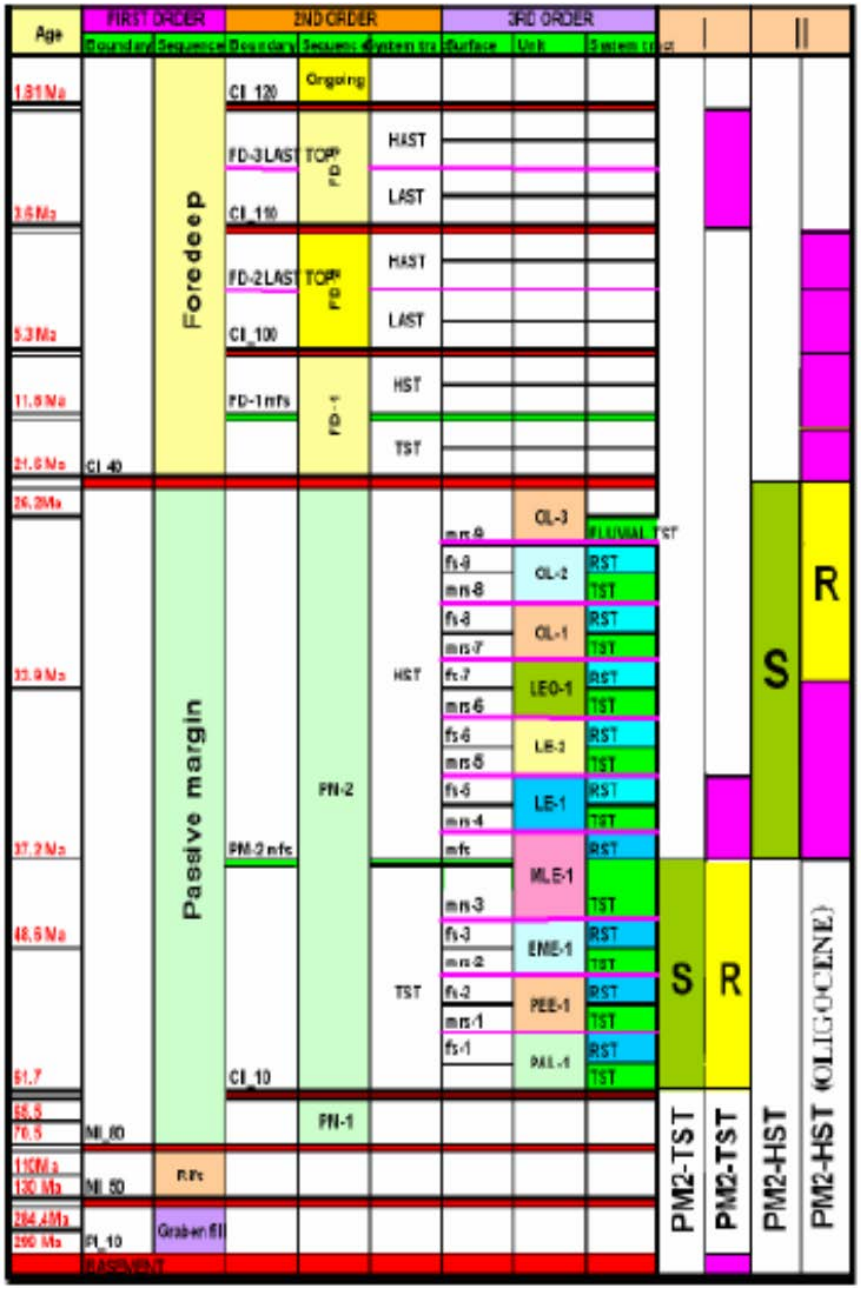

Figure 6. Sequence stratigraphy hierarchy of Assam and Assam Arakan Basin (after Singh et al., 2011).

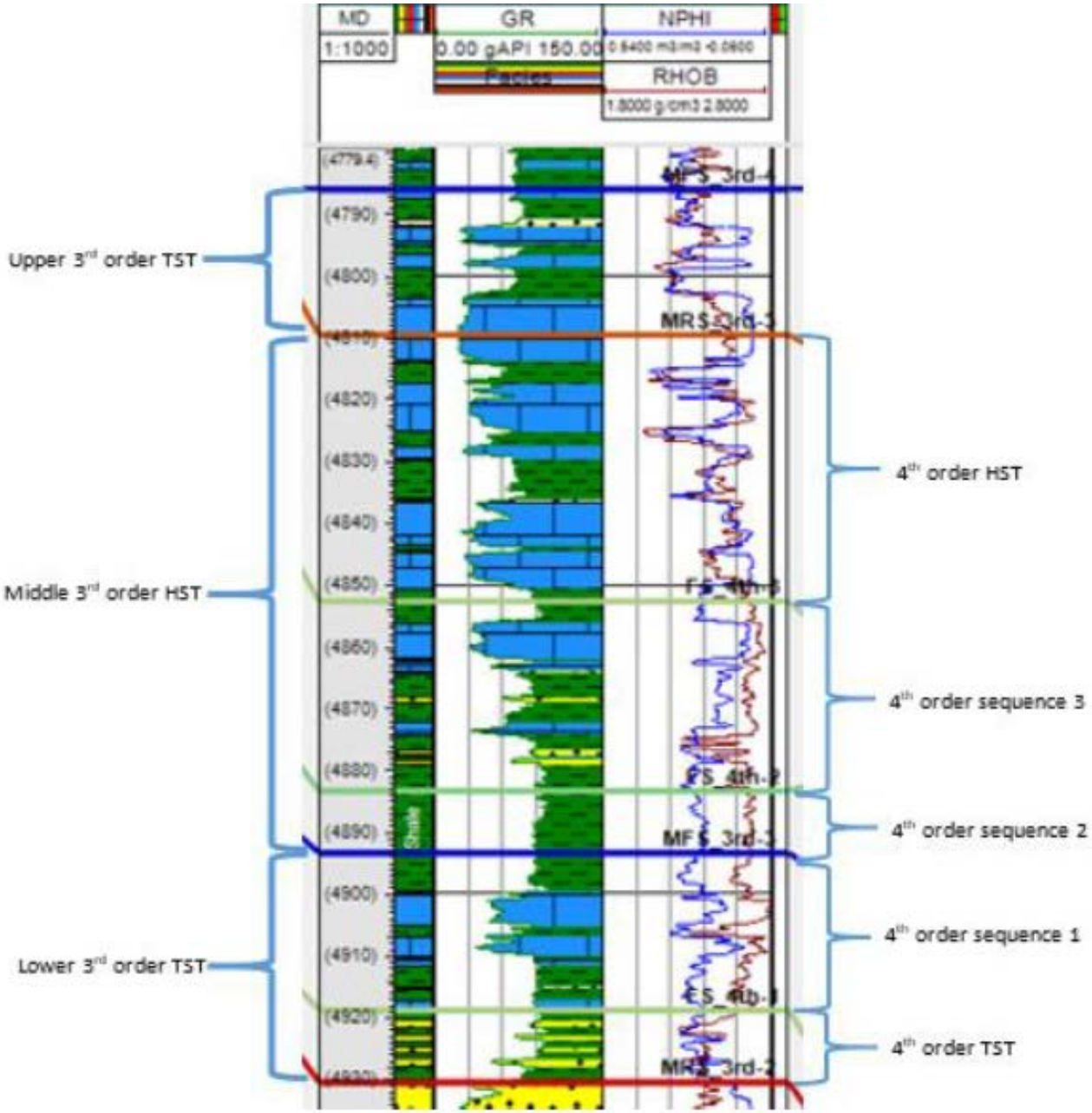

Figure 7. Key well showing lower order sequence stratigraphic surfaces within the 2nd order TST (see text for detail subdivision).

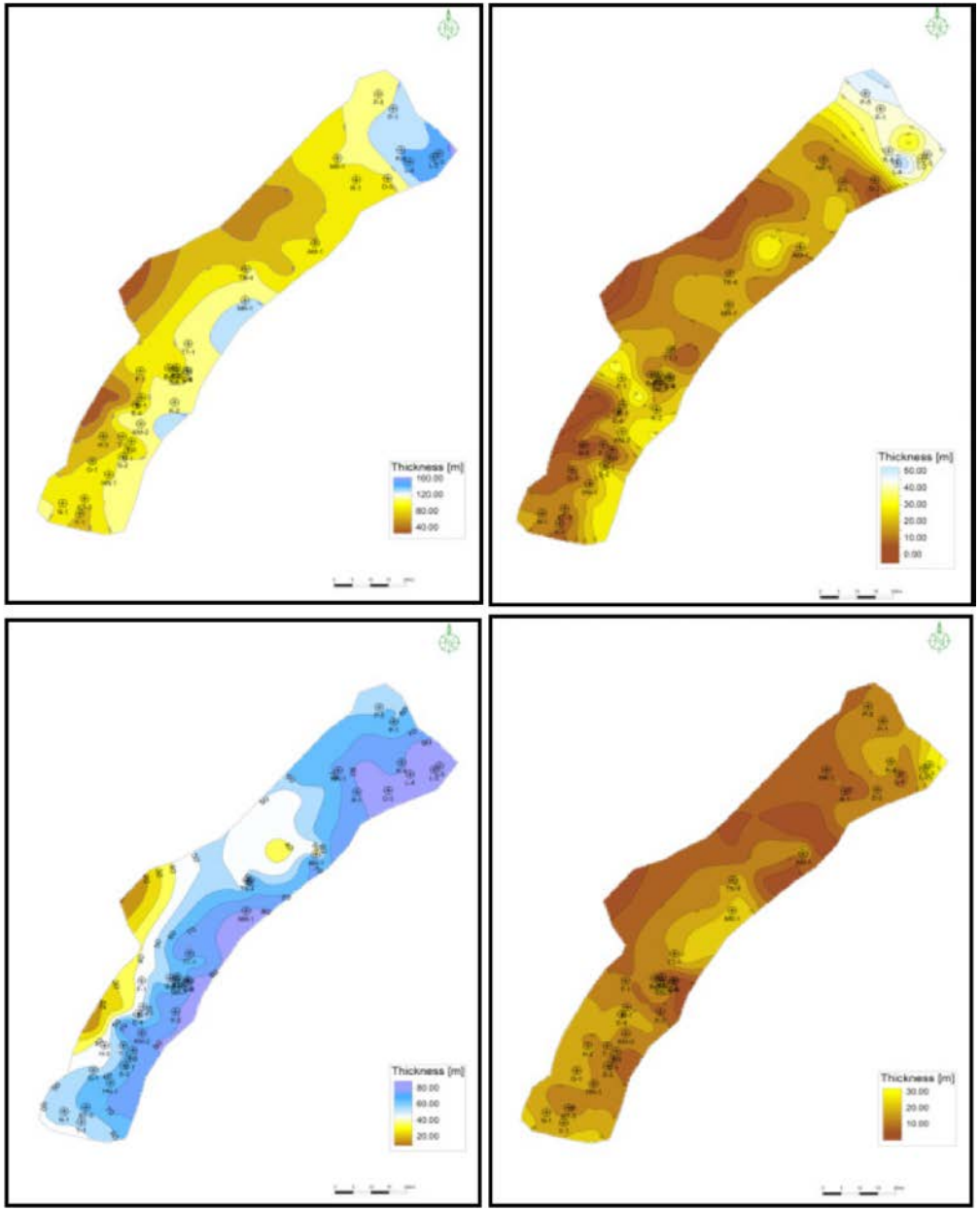

Figure 8. (a) Isopach map of total unit bounded by MRS_3rd-2 and MFS_3rd-4, (b) Isopach map of 3rd order upper TST, (c) Isopach map of 3rd order lower TST, (d) Isopach map of 3rd order middle HST.

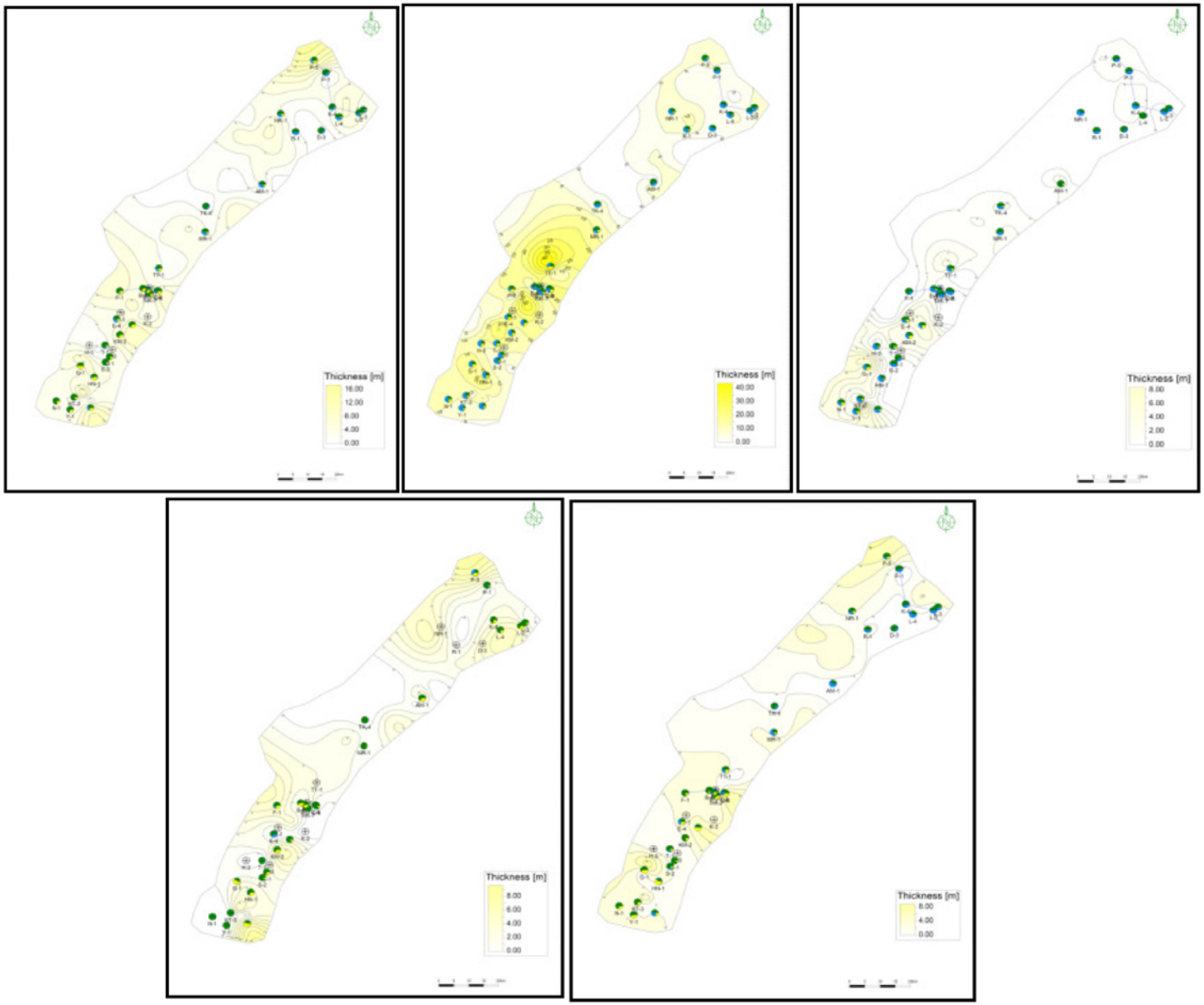

Figure 9. (a) Sand isolith map of 3rd order lower TST with pie diagram of facies proportions, (b) Sand isolith map of 3rd order middle HST with pie diagram of facies proportions, (c) Sand isolith map of 3rd order upper TST with pie diagram of facies proportions, (d) Sand isolith map of 4th order bottommost TST with pie diagram of facies proportions, (e) Sand isolith map of 4th order HST-TST unit-1

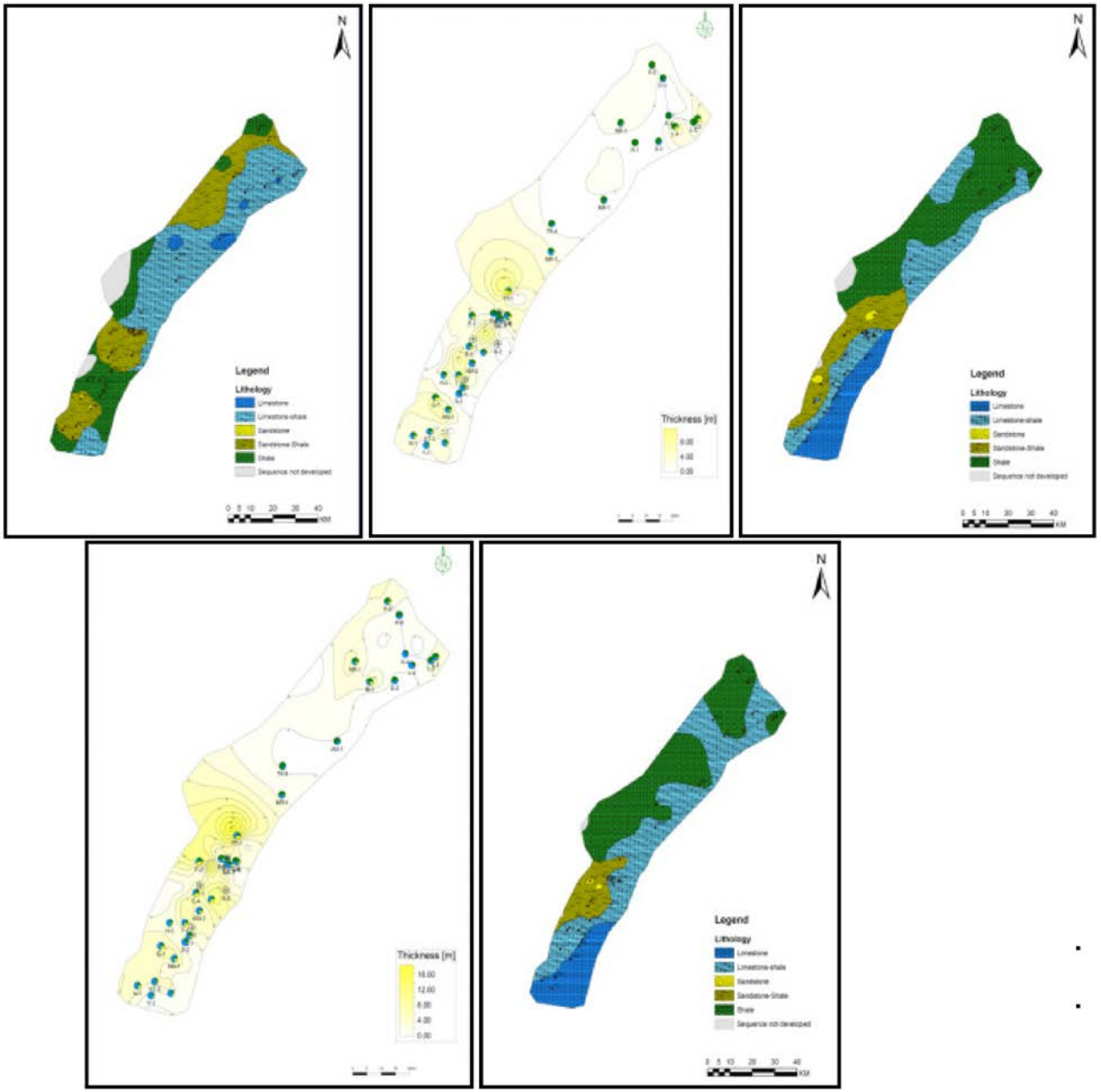

Figure 10. (a) Facies map of 4th order HST-TST unit-1, (b) Sand isolith of 4th order HST-TST unit-2, (c) Facies map of 4th order HST-TST unit-2, (d) Sand isolith map of 4th order HST-TST unit-3, (e) Facies map of 4th order HST-TST unit-3.

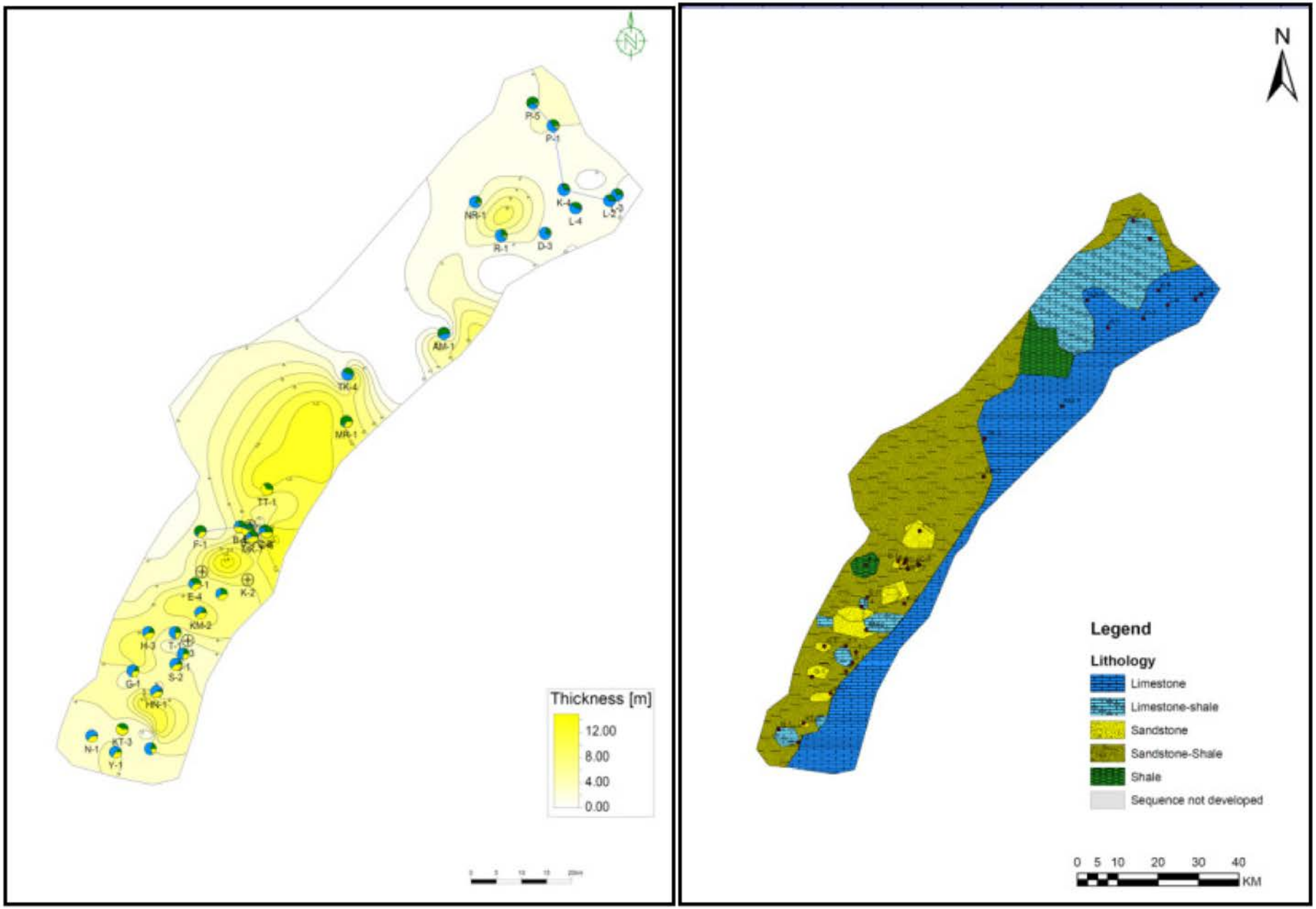

Figure 11. (a) Sand isolith map of 4th order top HST unit, (b) Facies map of 4th order top HST unit.

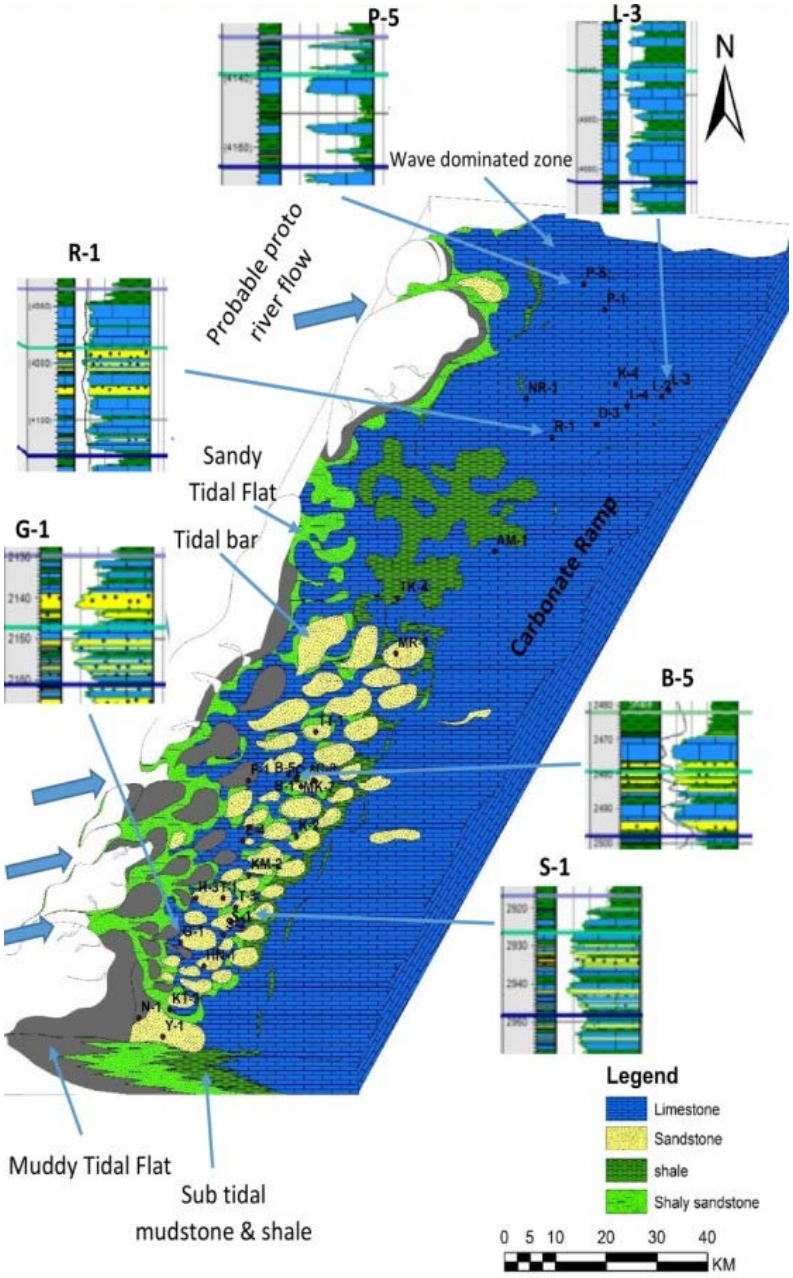

Figure 12. Depositional model of Sylhet Formation, Assam Shelf.

Figure 13. (a and b) Buff to dirty white micritic mudstone to wackestone (TST part), (c and d) Wackestone to packstone in the HST part, (e) Intraclastic limestone with rounded limestone fragments, (f and g) Low angle stylolitic laminae observed within Sylhet Formation.

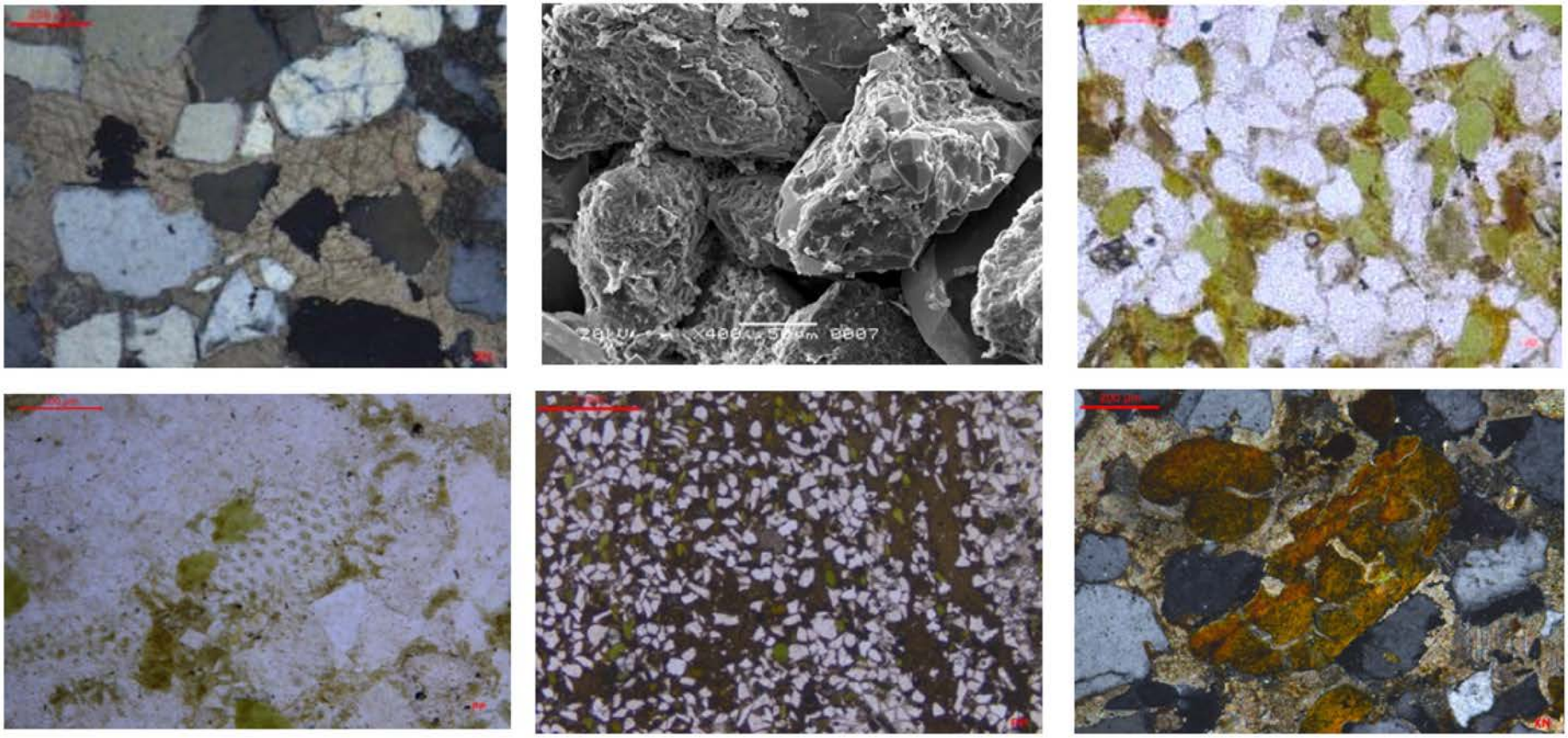

Figure 14. (a) Well C-8, Depth 2700.6m: Widespread early formed calcite cements with floating grains indicating eogenesis before compaction. Note etched grain boundary, (b) Well K-2, Depth 3323-3328m: SEM photomicrograph showing silica cementation in form of quartz overgrowth and some remnants of early calcite cements, (c) Well DM-3, Depth 3600-05m: Glauconitized quartz wacke showing line contact and glauconite pellets. Note most of the pellets are entire and fresh, (d) Well R-1, Depth 3685-90m: Fossil chamber filled with glauconites, (e) Well M-7, Depth 2836.8m: Glauconite occurrence as a cement, (f) Well M-7, Depth 2848.8m: Altered glauconite with deeply penetrating radiating cracks tapering inward.